High-Frequency MESFET Noise Modeling Including Distributed Effects

WOLFGANG HEINRICH, MEMBER, IEEE

Abstract—**A microwave FET noise analysis is presented including distributed effects caused by the wave propagation along the gate width direction. Using this model the noise characteristics of submicrometer-gate MESFET's at frequencies beyond 20 GHz are evaluated. We found that, in the case of well-designed quarter-micron LN-MESFET's, distributed effects may be neglected. Common lumped approximations, on the other hand, are shown to produce noticeable deviations. An improved lumped model is proposed.**

I. Introduction

THE RECENT improvements of the microwave FET frequency limits offer a great variety of new applications, especially in the low-noise field. State-of-the-art MESFET and HEMT devices achieve minimum noise figures of 2.5 and 2.4 dB at 35 and 60 GHz, respectively [1], [2].

Common small-signal models, on the other hand, cover only the frequency range up to about 20 GHz. For example, papers have been published recently discussing the influence of wave propagation along the electrodes [18], [19], and Oxley and Holden [20] propose that there may be a significant increase of the minimum noise figure due to such distributed effects. Thus the existing lumped models should be checked, and, if necessary, an extended FET description should be developed that holds well above 20 GHz.

In the following, some basic considerations on this topic will be presented. The paper concentrates on the question of how MESFET noise behavior can be modeled in the millimeter-wave range below 100 GHz, clarifying from a theoretical point of view

- whether distributed effects have to be accounted for;
- which elements should be added to the usual small-signal equivalent circuit;
- in which way the well-known $NF_{\min}$ formulas [5], [9] change.

As a consequence, a unit FET cell is studied (see Fig. 1) and any embedding or de-embedding problems will be excluded. One should note that the analysis presented can be employed also with HEMT devices when introducing adequate geometry and small-signal parameters.

Manuscript received February 9, 1988; revised December 6, 1988.

The author is with the Institut für Hochfrequenztechnik, Technische Hochschule Darmstadt, D-6100 Darmstadt, West Germany.

IEEE Log Number 8926572.

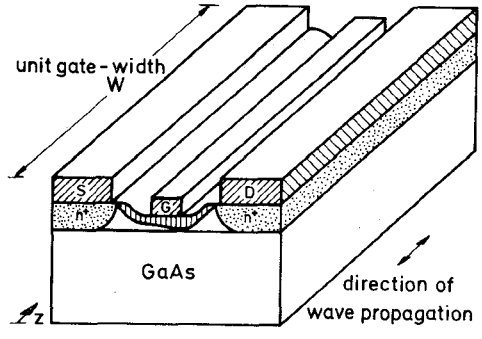

Fig. 1. Unit FET cell.

II. Method of Analysis

A. The Model

According to the aims outlined above, both wave propagation along the electrodes and the full small-signal equivalent circuit description of the intrinsic FET have to be included. Concerning the distributed phenomena, the present work is based on a fundamental field-theoretical analysis [10], which clearly indicates that the relevant wave modes are quasi-TEM ones and, hence, can be described by a distributed equivalent circuit formulation as demonstrated in [11] (for experimental data see [12]). These former treatments, however, employ a rather simplified description of the intrinsic FET and, therefore, have now been extended incorporating the full equivalent FET circuit and the noise generators, as shown in Fig. 2. Since we consider noise at small-signal operation in the microwave range, all the sources are assumed to produce pure diffusion noise.

In this context a few remarks are necessary on the contributions to MESFET noise theory published so far. To the knowledge of the author, van der Ziel performed the first specific investigations of MESFET noise [3], [4], assuming a relatively simple geometry and ohmic channel behavior. Pucel *et al.* [5] extended this treatment basically, introducing saturation effects by a two-region model. More recently, Cappy *et al.* [6]–[8] studied the noise in state-of-the-art FET structures employing a quasi-one-dimensional description that accounts for typical submicrometer-gate effects such as energy and momentum relaxation. Further-

0018-9480/89/0500-0836$01.00 ©1989 IEEE

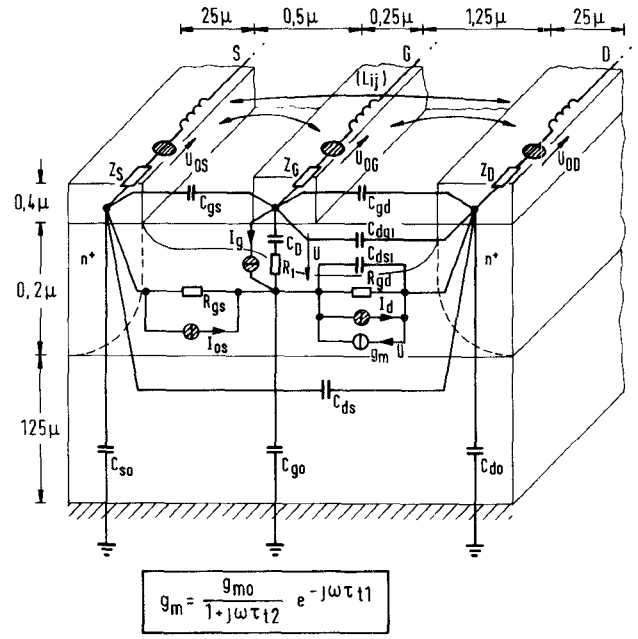

Fig. 2. The equivalent circuit model (all elements represent distributed quantities). The data employed for a typical 0.25-μm-gate MESFET are as follows:

Material constants: $\epsilon_r = 12.9$ for GaAs, electrode spacings filled with passivation layer ($\epsilon_r = 4$); electrode conductivity $\kappa = 4 \cdot 10^7\ (\Omega \cdot \mathrm{m})^{-1}$.
Intrinsic elements: (scaled to 300 μm gate width): $R_{gs} = 1\Omega$; $R_{gd} = 150\ \Omega$; $C_D = 0.22$ pF with $R_i C_D = \tau_i$ and $\tau_i = 0.4$ ps; $C_{dgi} = 0.015$ pF; $C_{dsi} = 0.04$ pF; $g_{m0} = 210$ mS/mm with $\tau_{t1} = 1.9$ ps and $\tau_{t2} = 0.1$ ps.
Noise sources: U_{0S}, U_{0G}, U_{0D}, I_{0S} are thermal noise generators;
$\langle I_g \cdot I_g^* \rangle = 4kT\Delta f \cdot \omega^2 C_D^2 / g_{m0} \cdot R$
$\langle I_d \cdot I_d^* \rangle = 4kT\Delta f \cdot g_{m0} \cdot P$
$\langle I_g^* \cdot I_d \rangle = 4kT\Delta f \cdot \omega C_D \cdot jC_{cor}\sqrt{RP}$
with $P = 1.1$, $R = 0.5$, and $C_{cor} = 0.7$ according to [8].

more, Fukui's work has to be mentioned. He approached the problem empirically and derived an approximate, but simple, formula [9], which is in widespread use.

One should outline that all these noise analyses assume quasi-static conditions. The drain–source current is set constant along the channel, thus neglecting any local splitting into a conductive part and a capacitive current flowing to the gate via the depletion layer at each point of the channel. As a consequence, for instance, both the charge resistor R_i and the transit time τ associated with the $e^{-j\omega\tau}$ term of g_m *cannot* be calculated using the theory of [3]–[8]. Concerning the noise quantities, these analyses fail in predicting higher order terms in ω for the parameters P, R, and C_{cor}. Therefore, the frequency dependence of P and C_{cor} as proposed by Cappy [8] seems to be questionable and is not considered throughout this paper (see also [21]).

Furthermore, it should be noted that the well-known NF_{min} derivation in [5] and, accordingly, Fukui's formulas [9] do *not* account for the transit time τ. Thus their validity is restricted to operation conditions where the effect of transit time on transconductance is negligible. Regarding typical quarter-micron-gate MESFET's with τ being in the range of 2 ps, however, this assumption holds only at relatively low frequencies ($\omega\tau \approx 0.25$ at 20 GHz). Hence, in the high-frequency regime, discrepancies due to the simplification in g_m can be expected (see subsection III-B).

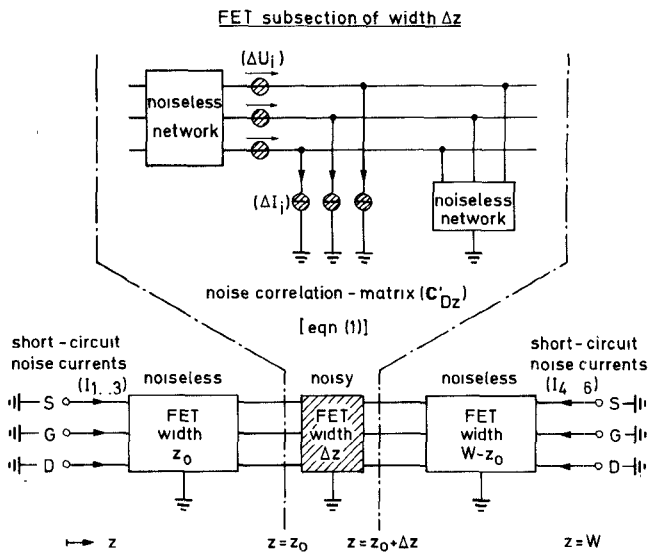

Fig. 3. The distributed noise analysis (see subsection II-B).

For the numerical calculations we choose typical element values according to measurement-fitted data from the literature or, if not available, to recent theoretical work [8], [13] (see Fig. 2). The stray capacitances, the electrode impedances, and the inductances are calculated from these data according to [11]. (For the gate electrode, for instance, an end-to-end resistance of about 250 Ω/mm is obtained.) Note that, concerning the expression for g_m, τ_{t2} is in general *not* equal to τ_i as set in the usual FET equivalent circuit (see [13]).

B. The Distributed Noise Analysis

For these studies it proves to be very useful to represent the noise quantities by their correlation matrices according to [14]. Fig. 3 explains the principle of the procedure.

We consider a noisy FET subsection of differential gate width Δz, located at $z = z_0$, which for $\Delta z \to 0$ may be described by means of lumped theory. In this way one derives the correlation matrix (C'_{Dz}):

$$(C'_{Dz}) = \frac{1}{\Delta z} \left\langle \begin{pmatrix} \Delta U_i \\ \vdots \\ \Delta I_i \\ \vdots \end{pmatrix} \cdot \begin{pmatrix} \Delta U_i \\ \vdots \\ \Delta I_i \\ \vdots \end{pmatrix}^{+} \right\rangle . \qquad (1)$$

The $\langle \cdots \rangle$ denote the mean fluctuations, the $+$ the transposed complex conjugate.

Note that C'_{Dz} is constant with z due to longitudinal homogeneity. The short-circuit noise currents at the outer ports of the transistor $(I_1 \cdots I_6)$ produced by the single FET subsection at z_0 can now be calculated assuming the remaining two sections of width z_0 and $W - z_0$ to behave as noiseless but distributed. This relation may be expressed

by the matrix $(A_{(z_0)})$:

$$\begin{pmatrix} I_1 \\ \vdots \\ I_6 \end{pmatrix} = (A_{(z_0)}) \cdot \begin{pmatrix} \Delta U_l \\ \vdots \\ \Delta I_l \\ \vdots \end{pmatrix}. \quad (2)$$

Consequently, one has the following expression for the current correlation matrix $(\Delta C_{(z_0)})$ related to the differential subsection of width Δz at $z = z_0$ (see Fig. 3):

$$(\Delta C_{(z_0)}) = \left\langle \begin{pmatrix} I_1 \\ \vdots \\ I_6 \end{pmatrix} \cdot \begin{pmatrix} I_1 \\ \vdots \\ I_6 \end{pmatrix}^+ \right\rangle \Bigg|_{\substack{\text{caused by noisy subsection} \\ \text{at } z = z_0}}$$

$$= (A_{(z_0)}) \cdot (C'_{Dz}) \cdot (A_{(z_0)})^+ \Delta z. \quad (3)$$

According to common noise theory [3]–[8], the noise generated by different FET subsections is uncorrelated. Therefore, the noise matrix (C_{tot}) of the whole FET can be evaluated by superposing all the contributions $(\Delta C_{(z_0)})$ of the sections at $z = z_{0l}$, which in the limiting case of $\Delta z \to 0$ leads to an integral expression:

$$(C_{\text{tot}}) = \sum_{l=1}^{N} (\Delta C_{(z_{0l})}) \to \int_{z_0=0}^{W} (A_{(z_0)}) \cdot (C'_{Dz}) \cdot (A_{(z_0)})^+ dz_0. \quad (4)$$

From (C_{tot}) all relevant quantities may be deduced according to common network noise theory.

It should be pointed out that for the distributed treatment described above no additional physical assumptions are required compared to previous lumped-element work [3]–[8]. In practice, the integral of (4) is solved numerically using a simple iterative trapezoidal rule.

III. Results and Discussion

A. Distributed Effects

Fig. 4 shows the gain and noise quantities of a quarter-micron-gate MESFET at 60 GHz. The different curves refer to lumped-element modeling and the two distributed configurations with input and output at the same end of the transistor and vice versa, respectively.

When increasing the unit gate width W for a given frequency, one observes successively two effects: first, the low-noise performance deteriorates (NF_{min} grows, G_{ass} and MAG decrease); second, deviations occur between the distributed and the corresponding lumped formulation due to wave propagation phenomena. This means in practice that whereas for LN MESFET's the unit gate width should be limited to relatively small values in order to avoid severe NF_{min} (and G_{ass}) deterioration, distributed effects do *not* play a significant role in such transistors!

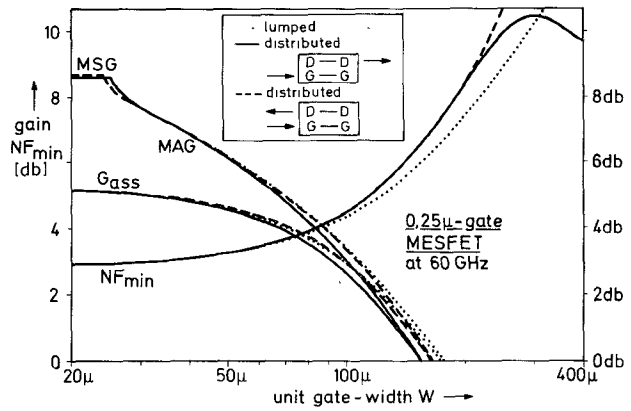

Fig. 4. MAG (MSG), minimum noise figure NF_{min}, and associated gain G_{ass} against unit gate width W at 60 GHz (0.25 μm-gate MESFET according to Fig. 2). Comparison between lumped model and distributed analysis applying the two different input–output configurations as indicated

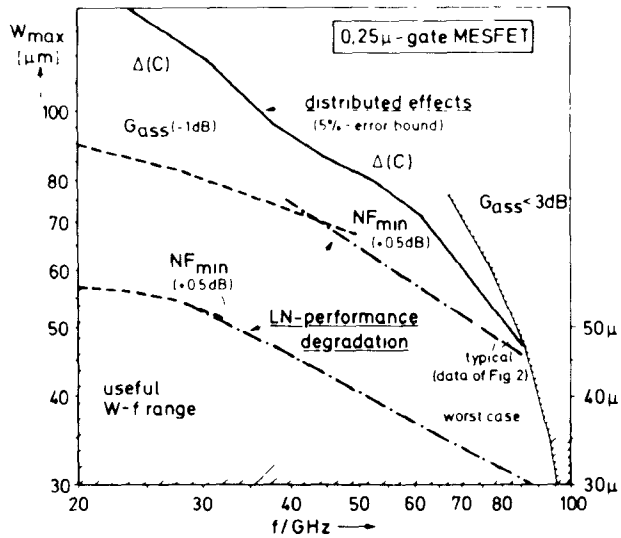

Fig. 5. Unit gate width limitations due to LN performance deterioration (NF_{min} and G_{ass}) and errors caused by distributed effects ($\Delta(C)$). $\Delta(C)$ denotes the maximum percentage of element error of the noise correlation matrix (C) (eq. (4)) weighted by the row-maximum. W_{max} is the maximum unit gate width dependent on the following restrictions: —— $\Delta(C)$ due to distributed effects exceeds 5 percent; ----- G_{ass} decrease >1 dB; —·—·— NF_{min} deterioration > 0.5 dB.

Fig. 5 illustrates these unit gate width limitations graphically. The results were obtained by a systematic investigation considering both input–output configurations, as indicated [15]. Because the FET parameters vary within a certain range, the diagram contains also the curves for the worst-case constellation. The above-mentioned observation is confirmed; i.e., lumped-element modeling holds well for well-designed 0.25-μm-gate LN-MESFET's, even at frequencies above 60 GHz. Additionally, Fig. 5 shows the useful range of unit width W. At 40 GHz, for instance, W should not exceed 40 μm. There exists, of course, a lower bound restriction on W as well. Given a total gate width the number of fingers should be small, since otherwise the parasitics of the feeding structures degrade noise characteristics.

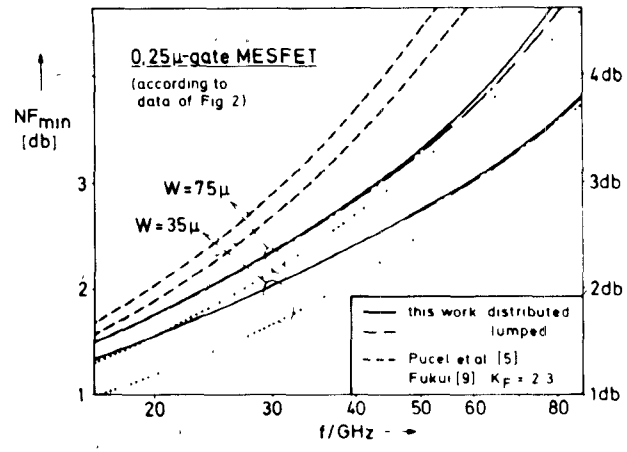

Fig. 6. NF_{min} against frequency with the unit gate width as parameter. Comparison between present analysis and the values calculated according to Pucel *et al.* [5] and Fukui [9]. The parameters introduced in the models [5], [9] correspond to those of Fig. 2 and are listed explicitly in the caption of Fig. 7.

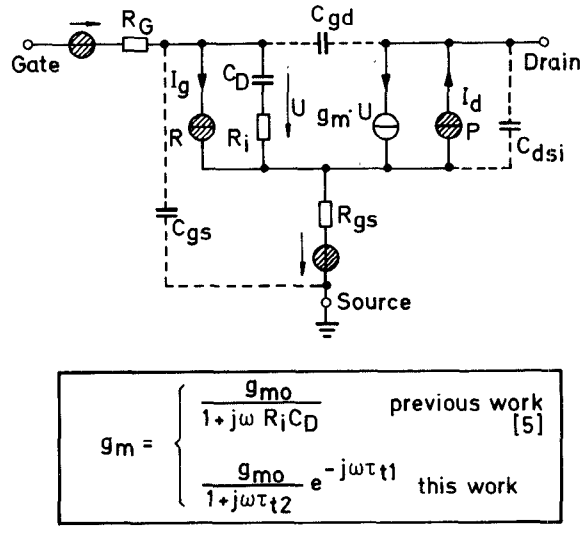

Fig. 7. Description of the noisy MESFET used by Pucel *et al.* [5] (solid lines) and the elements included additionally in this analysis (dotted). The network consists of lumped elements, whose values correspond to those of Fig. 2. They are as follows (except for R_G and g_{m0} all scaled to 300 μm gate width):

(i) Elements introduced into both the model of [5] and the new one: $R_G = 2.9\ \Omega$ for a single finger of 35 μm width; $C_D = 0.22$ pF with $\tau_i = R_i C_D = 0.4$ ps; $R_{gs} = 1\ \Omega$; $g_{m0} = 210$ mS/mm; $P = 1.1$; $R = 0.5$; $C_{cor} = C_{k0} = 0.7$ according to [8].

(ii) Additional elements which are accounted for by the new model; $\tau_{t1} = 1.9$ ps, $\tau_{t2} = 0.1$ ps, and thus $\tau_t = 2$ ps (see eq. (5)); $C_{gd} = 0.022$ pF; $C_{dsi} = 0.053$ pF; stray capacitance $C_{gs} = 0.016$ pF.

B. Improved Lumped-Element Modeling

According to the results of subsection A, a lumped-element description may be used in the frequency and gate width range of interest. As can be seen from Fig. 6, however, the model employed by Pucel *et al.* [5] (see Fig. 7) and the simple Fukui expression [9] give only a rather rough approximation. We found that the deviations compared to [5] are caused mainly by the g_m time constant τ_{t1} neglected there (see subsection II-A).

Furthermore, the feedback capacitance C_{gd} and the intrinsic element C_{dsi} are to be considered together with C_{gs} (see Fig. 7), which, however, is of minor influence. In our model C_{gs} describes the stray capacitance between source and gate electrodes, which gains in importance with decreasing gate length and spacing, providing T-shaped gates and depositing high-ϵ_r passivation layers (see also [22]). The drain resistance R_{gd}, on the other hand, turns out to be negligible.

C. The Minimum Noise Figure

The additional elements (see Fig. 7) require additional effort in calculating the minimum noise figure NF_{min}. The resulting formula is given in the Appendix.

For practical applications a power series expansion in ω offers advantages, since the mathematics simplify and the parameter dependences become more obvious. After a very lengthy but straightforward derivation one obtains for the complete model of Fig. 7

$$NF_{min} = 1 + \frac{2\omega C_D}{g_{m0}} \sqrt{P_0 R_0 (1 - C_{k0}^2) + g_{m0}\{P_0[R_G(1+\eta)^2 + R_s] - 2C_{k0}\sqrt{R_0 P_0}\,[R_G(1+\eta) + R_s] + R_0[R_G + R_s] + g_{m0} R_G R_s \eta^2\}}$$
$$+ 2\left(\frac{\omega C_D}{g_{m0}}\right)^2 g_{m0}\left\{P_0\left[R_G(1+\eta)^2 + R_s\left(1 + \frac{C_{gd}}{C_D}\right) + \frac{\tau_i}{C_D}\right] - C_{k0}\sqrt{R_0 P_0}\left[2(R_G(1+\eta) + R_s) + \frac{\tau_t}{C_D} + \frac{C_{gd}}{C_D}\left(R_s + \frac{1}{g_{m0}}\right)\right]\right.$$
$$\left. - \frac{C_{k1}}{C_D}\sqrt{R_0 P_0} + R_0[R_G + R_s] + R_s\left(g_{m0} R_G \eta^2 - \frac{C_{gd} + C_{dsi}}{C_D}\right)\right\}$$
$$+ \text{higher order terms} \cdots \tag{5}$$

Fig. 7 shows the extended model that will be used for the following derivations of NF_{min}. One should note that both this description and the previous one [5] are based on the same well-known small-signal equivalent circuit. The only difference is that the model presented here accounts for additional elements of this circuit (i.e., C_{gd}, C_{dsi}, and τ), which were neglected in the previous treatments.

with (see Fig. 2)

$$\eta = \frac{C_{gs} + C_{gd}}{C_D}$$
$$P = P_0 + \omega^2 P_1 + \cdots$$
$$R = R_0 + \omega^2 R_1 + \cdots$$
$$C_{cor} = C_{k0} + j\omega C_{k1} + \omega^2 C_{k2} + \cdots$$
$$g_m = g_{m0}(1 - j\omega\tau_t + \cdots)$$
$$\tau_t = \tau_{t1} + \tau_{t2}.$$

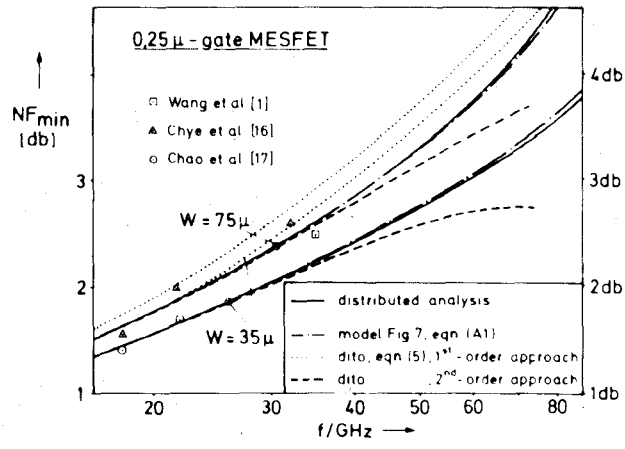

Fig. 8. $NF_{\min}$ against frequency. Curves of Fig. 6 using the improved $NF_{\min}$ formulas of (5) and (A1), respectively. Additionally, experimental data from the literature are shown.

Fig. 8 demonstrates the excellent agreement between the improved lumped model (eq. (A1)) and the distributed analysis. Note that the previous formula according to [5] results in a deviation of about 1.5 dB at 60 GHz. The diagram also contains experimental data from the literature [1], [16], [17].

In general, any first-order approximation in ω leads to questionable results in the frequency range above 20 GHz, whereas the second-order approach of (5) holds well up to about 50 GHz. Beyond this limit third-order terms would have to be included, which, however, cause additional efforts that do not seem to be justified when compared to the "exact" formula given in (A1).

For $\tau_t = \tau_i$, $C_{gd} = C_{dsi} = C_{gs} = 0$, and thus $\eta = 0$, (5) reduces to the well-known formula derived by Pucel *et al.* [5]. Regarding state-of-the-art FET's, however, the assumption $\tau_t = \tau_i$ does not hold. The τ_t values measured are considerably larger than those of τ_i. Then the ω^2 coefficient in (5) is dominated by the term τ_t/C_D, thus reducing the $NF_{\min}$ value due to its negative sign. Quantitatively, this contribution of the ω^2 term is relatively large, so that it remains remarkable even at the lower frequency end of Fig. 6.

On the other hand, the capacitances C_{gd}, C_{dsi}, and C_{gs} needs special consideration in the case of submicron-gate FET's. Reducing the gate length, the depletion-layer capacitance C_D decreases whereas C_{gd}, C_{dsi}, and the stray capacitances increase depending on the reduced dimensions. Thus the terms C_{gd}/C_D, C_{dsi}/C_D, and $\eta = (C_{gs} + C_{gd})/C_D$ become of particular importance at small gate lengths (e.g.: $\eta = 0.17$ assuming the data of Fig. 7). Note that this characteristic depends primarily on the submicron geometry and not on the frequency of operation.

Furthermore, one should note that the first-order term C_{k1} of the correlation factor may change the $NF_{\min}$ value, too, whereas the higher order terms P_1, R_1, and C_{k2} do not appear (see (5)). To date, however, there are no reliable results on C_{k1} available, because all approaches known to the author (e.g. [3]–[9]) assume quasi-static conditions (see subsection II-A).

In summarizing, one can state that the drift time τ_t and the intrinsic capacitance C_{dsi} *reduce* the value of $NF_{\min}$. Assuming typical MESFET parameters, this is true for the feedback capacitance C_{gd} as well. The stray capacitance C_{gs}, on the other hand, causes a slight $NF_{\min}$ increase, which disappears for small R_G. The drift time τ_t exerts the strongest influence on $NF_{\min}$. Therefore, a considerable improvement over [5] is achieved when accounting only for $\tau_t \neq \tau_i$ and setting $C_{gd} = C_{dsi} = C_{gs} = 0$. Equation (5) then simplifies to the expression of (6). Note that its first-order term in frequency is identical to that given in [5]:

$$NF_{\min} = 1 + \frac{2\omega C_D}{g_{m0}} \sqrt{P_0 R_0 (1 - C_{k0}^2) + g_{mo}(R_G + R_s)\left(P_0 - 2C_{k0}\sqrt{R_0 P_0} + R_0\right)}$$
$$+ 2\left(\frac{\omega C_D}{g_{m0}}\right)^2 g_{m0} \cdot \left\{ (R_G + R_s)\left(P_0 - 2C_{k0}\sqrt{R_0 P_0} + R_0\right) \right.$$
$$\left. + P_0 \frac{\tau_i}{C_D} - C_{k0}\sqrt{R_0 P_0}\,\frac{\tau_t}{C_D} - \frac{C_{k1}}{C_D}\sqrt{R_0 P_0} \right\}. \quad (6)$$

IV. Conclusions

Extrapolating the MESFET characteristics from frequencies below 20 GHz to the millimeter-wave range, one concludes with regard to small-signal noise modeling:

- For state-of-the-art LN devices, no distributed description is required. Unit gate width, on the other hand, has to be kept small enough to maintain the desired LN properties (for data, see Fig. 5).
- The FET equivalent circuit approximations used previously (e.g. [5]) give only poor accuracy in the high-frequency range. Additional elements should be included, in particular the g_m drift time τ_t and, if necessary, the capacitances C_{gd} and C_{dsi} (see Fig. 7).

A FET model extended in this way gives theoretically accurate $NF_{\min}$ values even at frequencies above 60 GHz. The second-order expansion in ω provides reliable results in the lower range up to about 50 GHz. Equations (A1), (5), and (6) contain the corresponding mathematics. Any first-order approximation leads to noticeable deviations.

The investigations point out the significance of the different time constants and higher order frequency terms such as τ_t and C_{k1} on high-frequency FET characteristics. Unfortunately, the theoretical approaches to a submicrometer FET description that are available are based on

quasi-static assumptions and, hence, cannot provide these values. Therefore, a nonstatic small-signal analysis of such FET's that includes not only relaxation effects [6]–[8] but also time harmonic steady-state conditions is to be encouraged.

Appendix

The minimum noise figure of the complete model shown in Fig. 7 may be written as follows (note that, in general, the noise parameters P, R and C_{cor}, given by Fig. 2, are frequency dependent and C_{cor} is a complex number):

$$NF_{min} = 1 + 2R_N\left(G_K + \sqrt{G_K^2 + \frac{G_N}{R_N}}\right) \tag{A1}$$

with

$$R_N = \frac{1}{|c|^2} N_{22}$$

$$G_N = \frac{\omega^2 C_D^2}{|b|^2}\left\{N_{11} - \frac{1}{N_{22}}|N_{12}|^2\right\}$$

$$G_K = \omega C_D \cdot \mathrm{Im}\left\{\frac{1}{b}\left(c\frac{N_{12}}{N_{22}} - a\right)\right\}$$

$$N_{11} = R_G|a|^2 + \frac{1}{R_s}|g|^2 + \frac{R}{g_{m0}}|h|^2 + g_{m0}|g|^2 P - 2\sqrt{RP}\,\mathrm{Re}\{C_{cor} g h^*\}$$

$$N_{22} = R_G|c|^2 + \frac{1}{R_s}|d|^2 + \omega^2 C_D^2 |e|^2 \frac{R}{g_{m0}} + g_{m0}|f|^2 P + 2\omega C_D\sqrt{RP}\,\mathrm{Im}\{e^* f C_{cor}\}$$

$$N_{12} = R_G a c^* + \frac{1}{R_s} g d^* + C_{cor}^*\sqrt{RP}\, h f^* - g_{m0} P g f^* + j\omega C_D\left[g e^* C_{cor}\sqrt{RP} - \frac{R}{g_{m0}} h e^*\right]$$

$$a = Y_1\frac{1}{1 + j\omega\tau_t} + \frac{C_{gs} + C_{gd}}{C_D}(Y_1 + Y_2)$$

$$b = R_G\{(Y_1 + Y_2)Y_3 + Y_1 Y_e\}$$

$$c = g_m Y_1 - j\omega\left[C_{dsi} Y_2 + C_{gd}(Y_1 + Y_2)\right]$$

$$d = R_G\left\{g_m Y_3 + j\omega\left[C_{dsi}(Y_e + Y_3) + C_{gd} Y_e\right]\right\}$$

$$e = (-R_G)\left\{g_m(Y_1 + Y_3) + j\omega\left[C_{dsi} Y_3 - C_{gd}(Y_1 + g_m)\right]\right\}$$

$$f = R_G\left\{\frac{1}{R_s}(Y_e + Y_3) + Y_e\left(\frac{1}{R_G} + j\omega C_{gs}\right)\right\}$$

$$g = \frac{1}{1 + j\omega\tau_t}$$

$$h = Y_1 + g_m$$

$$Y_1 = \frac{1}{R_s} + j\omega C_{dsi}$$

$$Y_2 = Y_e + g_m$$

$$Y_3 = \frac{1}{R_G} + j\omega(C_{gs} + C_{gd})$$

$$Y_e = j\omega C_D \frac{1}{1 + j\omega\tau_t}$$

$$g_m = g_{m0}\frac{1}{1 + j\omega\tau_{t2}} e^{-j\omega\tau_{t1}}.$$

R_N, G_N, G_K, N_{11}, and N_{22} are real numbers; the remaining quantities in (A1) are complex. For the circuit elements, please refer to Fig. 7.

Acknowledgment

The author is indebted to Dr. H. L. Hartnagel for his continuous encouragement and for a first review of this paper. Thanks are also due to Dr. A. Cappy from Lille, France, for helpful discussions and for providing a preprint of his recent paper. Last but not least, S. Matthäus and A. Hoge should be mentioned for their efforts on editing the manuscript.

References

[1] K.-G. Wang and S.-G. Wang, "State-of-the-art ion-implanted low-noise GaAs MESFET's and high-performance monolithic amplifiers," *IEEE Trans. Electron Devices*, vol. ED-34, pp. 2610–2615, 1987.

[2] P. C. Chao *et al.*, "0.1 μm gate-length pseudomorphic HEMT's," *IEEE Electron Device Lett.*, vol. EDL-8, pp. 489–491, 1987.

[3] A. van der Ziel, "Thermal noise in field-effect transistors," *Proc. IRE*, pp. 1808–1812, Aug. 1962.

[4] A. van der Ziel, "Gate noise in field effect transistors at moderately high frequencies," *Proc. IRE*, pp. 461–467, Mar. 1963.

[5] R. A. Pucel, H. A. Haus, and H. Statz, "Signal and noise properties of gallium arsenide microwave field-effect transistors," in *Advances in Electronics and Electron Physics*, vol. 38. New York: Academic press, 1975, pp. 195–265.

[6] B. Carnez, A. Cappy, R. Fauquembergue, E. Constant, and G. Salmer, "Noise modeling in submicrometer-gate FET's," *IEEE Trans. Electron Devices*, vol. ED-28, pp. 784–789, 1981.

[7] A. Cappy, A. Vanoverschelde, M. Schortgen, C. Versnaeyen, and G. Salmer, "Noise modeling in submicrometer-gate two-dimensional electron-gas field-effect-transistors," *IEEE Trans. Electron Devices*, vol. ED-32, pp. 2787–2795, 1985.

[8] A. Cappy, "Noise modeling and measurement techniques," *IEEE Trans. Microwave Theory Tech.*, vol. MTT-36, pp. 1–10, 1988.

[9] H. Fukui, "Optimal noise figure of microwave GaAs MESFET's," *IEEE Trans. Electron Devices.*, vol. ED-26, pp. 1032–1037, 1979.

[10] W. Heinrich and H. L. Hartnagel, "Wave propagation on MESFET electrodes and its influence on transistor gain," *IEEE Trans. Microwave Theory Tech.*, vol. MTT-35, pp. 1–8, 1987.

[11] W. Heinrich, "Distributed equivalent-circuit model for Traveling-wave FET design," *IEEE Trans. Microwave Theory Tech.*, vol. MTT-35, pp. 487–491, 1987.

[12] K. Fricke and W. Heinrich, "Measurement of GaAs-MESFET distributed properties," *Arch. Elek. Übertragung*, vol. 42, pp. 260–261, 1988.

[13] M. B. Das, "Millimeter-wave performance of ultra-submicrometer-gate field-effect transistors: A comparison of MODFET, MESFET and PBT structures," *IEEE Trans. Electron Dev.*, vol. ED-34, pp. 1429–1440, 1987.

[14] H. Hillbrand and P. H. Russer, "An efficient method for computer aided noise analysis of linear amplifier networks," *IEEE Trans. Circuits Syst.*, vol. CAS-23, pp. 235–238, 1976.

[15] W. Heinrich, "Distributed analysis of submicron-MESFET noise-

properties," in *IEEE MTT-S Int. Microwave Symp. Dig.*, 1988, pp. 327–330.

[16] P. W. Chye and C. Huang, "Quarter micron low-noise GaAs FET's," *IEEE Electron Device Lett.*, vol. EDL-3, pp. 401–403, 1982.

[17] P. C. Chao, P. M. Smith, S. C. Palmateer, and J. C. Hwang, "Electron-beam fabrication of GaAs low-noise MESFET's using a new trilayer resist technique," *IEEE Trans. Electron Devices*, vol. ED-32, pp. 1042–1046, 1985.

[18] G. Ghione and C. U . Naldi, "Modeling and simulation of wave propagation effects in MESFET devices based on physical models," in *Proc. 17th European Solid State Device Res. Conf.* (Bologna, Italy), 1987, pp 317–320.

[19] L. Escotte, J. C. Mollier, and M. Lecreff, "Noise and small-signal distributed model of mm-wave FETs," in *IEEE MTT-S Int. Microwave Symp. Dig.*, 1988, pp. 919–922.

[20] C. H. Oxley and A. J. Holden, "Simple models for high-frequency MESFETs and comparison with experimental results," *Proc. Inst. Elec. Eng.*, vol. 133, pt. H, pp. 335–340, 1986.

[21] A. Cappy and W. Heinrich, "The high frequency FET noise performance: A new approach," *IEEE Trans. Electron Devices*, to be published.

[22] T. Enoki, K. Yamasaki, K. Osafune, and K. Ohwada, "0.3 μm advanced SAINT FET's having asymmetric n^+-layer for ultra-high-frequency GaAs MMIC's," *IEEE Trans. Electron Devices*, vol. ED-35, pp. 18–24, 1988.

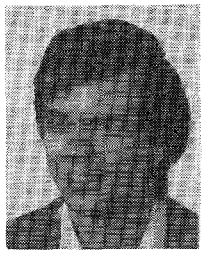

Wolfgang Heinrich (M'84) was born in Frankfurt am Main, West Germany, in 1958. He received the Dipl.-Ing. and Dr.-Ing. degrees from the Technical University of Darmstadt, West Germany, in 1982 and 1987, respectively.

In 1983, he joined the Institut für Hochfrequenztechnik of the same university, where he is currently engaged in FET noise modeling and field-theoretical investigations of planar transmission lines.